

CuO and MoS₂ difference including S -rGO and PPy nanocomposite for SupercapBattery device

Murat Ates*

¹Department of Chemistry /Faculty of Arts and Sciences, Tekirdag Namik Kemal University, Turkiye

*(mates@nku.edu.tr) Email of the corresponding author

Abstract – In this study, electrochemical performances of Copper (II) oxide (CuO) and Molybdenum (IV) sulfide (MoS₂) were comparatively investigated by cyclic voltammetry (CV), galvanostatic charge discharge (GCD) and electrochemical impedance spectroscopy (EIS) measurements. We have designed SupercapBattery with Al and Cu electrodes on 2032 coin cell. Ionic liquid (1-butyl-3-methylimidazolium tetra fluoroborate) was used to carry out electrolyte between the anode and cathode compartments. The highest specific capacitance was obtained as $C_{sp} = 1110.32 \text{ F} \times \text{g}^{-1}$ at $2 \text{ mV} \times \text{s}^{-1}$ by CV method for S-rGO/MoS₂/PPy nanocomposite. CuO was seriously reduced the electrochemical performances of SupercapBattery device ($C_{sp} = 113.10 \text{ F} \times \text{g}^{-1}$ at $2 \text{ mV} \times \text{s}^{-1}$ by CV method) for S-rGO/CuO/PPy nanocomposite. (Electrode weights were obtained as 19.8 mg and 21.8 mg for S-rGO/MoS₂/PPy and S-rGO/CuO/PPy nanocomposites, respectively).

Keywords – S-rGO, SupercapBattery, CuO, Polypyrrole, Nanocomposite, MoS₂

I. INTRODUCTION

In this study, a new design of hybrid anode and cathode materials were used as an electrode materials. We have comparatively investigated MoS₂ and CuO metal oxides with S doped rGO (S-rGO) and polypyrrole (PPy).

Nowadays, supercapacitors are used as a new kind of energy storage system for renewable power generation and electric vehicles etc. [1-3]. Supercapacitors facilitate fast charge/discharge, high energy and power density devices [4], and thus the electrode properties, such as nature of the active materials, specific surface area, pore-size distribution etc., are key for ensuring excellent supercapacitor performances [5-7].

Metal oxides are synthesized for porous and nanostructures. Electrode materials affect the electrochemical performances of SupercapBattery devices. There are many factors for this influence, such as wide surface areas, big pore sizes and good electrical conductivity. Therefore, they are excessively used in harvesting and energy storage

systems including batteries and supercapacitors [8-10].

Among many carbon-based nanostructured materials, graphene as a single-atom thick sheet of hexagonally arrayed sp²-bonded carbon atoms has been used for supercapacitor applications owing to its extraordinary electronic, thermal and mechanical properties as well as its high surface area ($2630 \text{ g} \times \text{m}^{-2}$) and chemical stability [11-14]. In this study, we used MoS₂ and CuO metal oxides with S-doped rGO and PPy materials.

II. MATERIALS AND METHOD

Electrochemical measurements were performed with 2032 coin-type cells. The slurry was obtained by mixing the as-synthesized materials, acetylene black and N-methyl-2-pyrrolidone (NMP) as a solvent for materials. Polyvinyl pyrrolidone (PVP) was performed by binder. Then the slurry was pasted onto Al and Cu foils and dried at 60 °C in a vacuum oven for 12 h. The electrolyte was ionic liquid (IL). Galvanostatic charge/discharge, rate

performance and cyclic performances were tested between 0.0 and 0.8 V by using ivium-vertex potentiostat-galvanostat instrument. Electrochemical impedance spectroscopy (EIS) was taken from 10 mHz to 100 kHz using 10 mV amplitude.

A. S-rGO synthesis

In literature, the conductivity of GO increases by doped of S and N elements [15, 16]. As a result, S doped GO have a superior performance compared to other additives (N, B or P) in terms of capacitor performance [17]. 5 ml Na₂S was mixed in various sources (0.5 M). It was synthesized in a microwave oven at 180 Watt and 20 min. So, S-GO was obtained by centrifuged 3 times [18].

B. Metal oxides (MoS₂ and CuO)

Sodium molybdate (VI) dehydrate (NaMoO₄×2H₂O, 0.0053 g) and thiourea (H₂NCSNH₂, 0.9453 g) were dissolved in deionized (DI) water (33 ml). The mixture was transferred to a hydrothermal synthesis reactor for 24 h at 210 °C. The precipitate was removed and immersed in DI water and sonicated for 30 min. Excess impurities was removed from the mixture by centrifugation 5 times at 6000 rpm for 15 min. Thus, MoS₂ nanomaterial was synthesized the above procedure [19].

Copper oxide (CuO) is a well-known transition metal oxide, which has many crystal forms [19]. It has been used in supercapacitors due to their unique advantages of low cost, high chemical stability, and good electrochemical performances [20]. Moreover, They have also abundant resources, non-toxicity and easy tailoring of various shapes [21, 22]. In literature, there are a lot of works on controllable synthesis of copper oxide nanoparticles [23-25].

C. Polypyrrole (PPy)

Polypyrrole was synthesized by chemical oxidation polymerization method. Pyrrole monomer, potassium dichromate (K₂Cr₂O₇) was used as oxidizer and H₂SO₄ as additive. Chemical polymerization was carried out by adding 1 M H₂SO₄ and 1 M pyrrole monomer solution dropwise addition to the above solution. Polymerization was carried out with constant stirring for 24 h with ice-bath condition. After the obtained product was filtered and washed with DI water. The black

colored PPy powders were dried in an oven at 100 °C for 1.5 h [26].

III. RESULTS & DISCUSSION

D. SEM-EDX analysis

The SEM images of GO, S-rGO, MoS₂ and PPy were shown in Figure 1. There were flat surfaces of materials without reduction process of GO like Fig.1a.

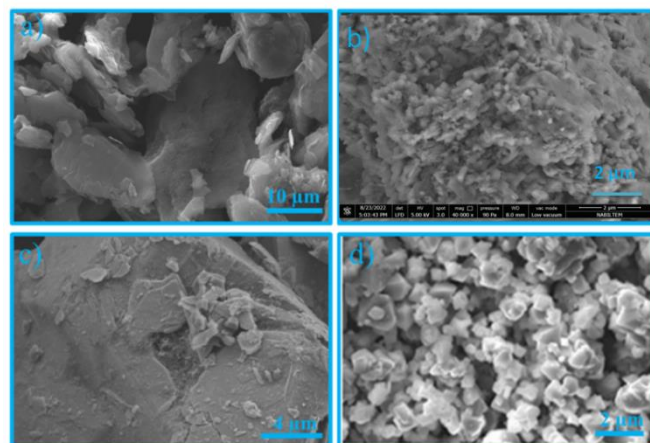


Figure 1. SEM images of a) GO, b) S-rGO, c) MoS₂, d) PPy.

The EDX mapping analysis of GO, S-rGO, MoS₂, and PPy materials were presented in Fig.2. The reduction of GO was supported by EDX analysis. The evidence of successful synthesis of materials was given for % elements of S, C, Mo, O and N in the nanocomposite structures.

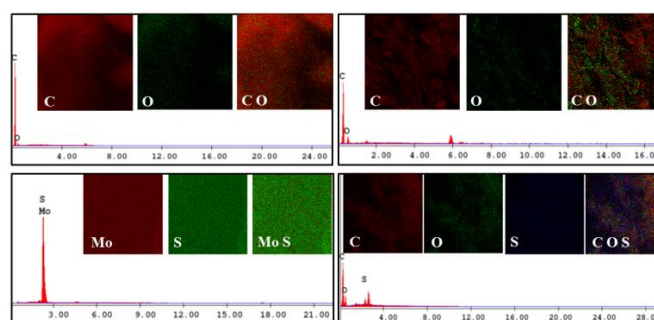


Figure 2. EDX mapping analysis of GO, S-rGO, c) MoS₂, d) PPy.

E. Electrochemical performances of SupercapBattery device

S-rGO/CuO/PPy and S-rGO/MoS₂/PPy nanocomposites were measured by CV, GCD and EIS measurements.

F. CV measurements

CV plots of S-rGO/CuO/PPy and S-rGO/MoS₂/PPy nanocomposites at different scan rates from 1000 mV×s⁻¹ to 2 mV×s⁻¹ were given in Figure 3.

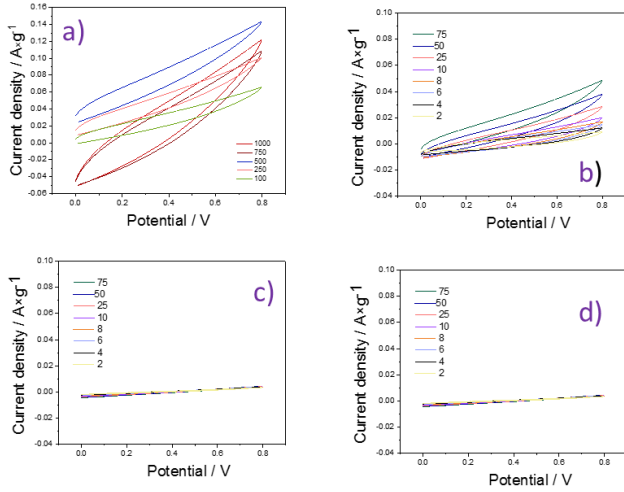


Fig. 3 CV plots of S-rGO/MoS₂/PPy nanocomposite at different scan rates, a) 1000-100 mV×s⁻¹, b) 75-2 mV×s⁻¹. S-rGO/CuO/PPy nanocomposite at different scan rates, c) 1000-100 mV×s⁻¹, d) 75-2 mV×s⁻¹.

The lowest specific capacitance was obtained as $C_{sp} = 17.02 \text{ F} \times \text{g}^{-1}$ at 1000 mV×s⁻¹ for S-rGO/MoS₂/PPy nanocomposite. However, the highest specific capacitance was found as $C_{sp} = 1110.32 \text{ F} \times \text{g}^{-1}$ at 2 mV×s⁻¹ for S-rGO/MoS₂/PPy nanocomposite. There is a logarithmic decrease by increasing of scan rate due to fast ion movement from one compartment to another compartment (Figure 3).

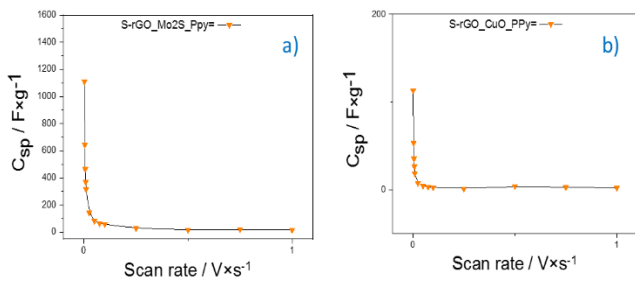


Fig. 4 C_{sp} vs. Scan rate plot of a) S-rGO/MoS₂/PPy nanocomposite, b) S-rGO/CuO/PPy nanocomposite.

G. GCD measurements

GCD plots of S-rGO/CuO/PPy and S-rGO/MoS₂/PPy nanocomposites were given at constant current density from 0.1 A×g⁻¹ to 10 A×g⁻¹ as shown in Figure 5. The highest specific capacitance was obtained as $C_{sp} = 2.36 \text{ F} \times \text{g}^{-1}$ at 0.1 mA for S-rGO/MoS₂/PPy nanocomposites and $C_{sp} =$

2.58 F×g⁻¹ at 0.1 mA for S-rGO/CuO/PPy nanocomposite by GCD measurements.

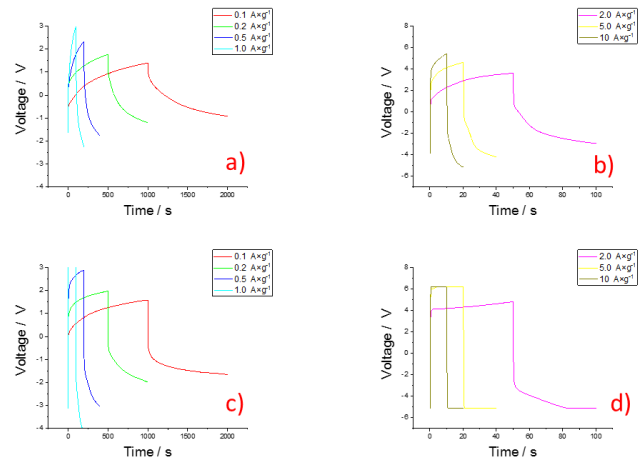


Fig. 5 GCD plots of S-rGO/MoS₂/PPy nanocomposite at constant current density from a) 0.1 A×g⁻¹ to 1 A×g⁻¹, b) 2.0 A×g⁻¹ to 10 A×g⁻¹ and S-rGO/CuO/PPy nanocomposite at constant current density from c) 0.1 A×g⁻¹ to 1 A×g⁻¹, d) 2.0 A×g⁻¹ to 10 A×g⁻¹.

H. EIS measurements

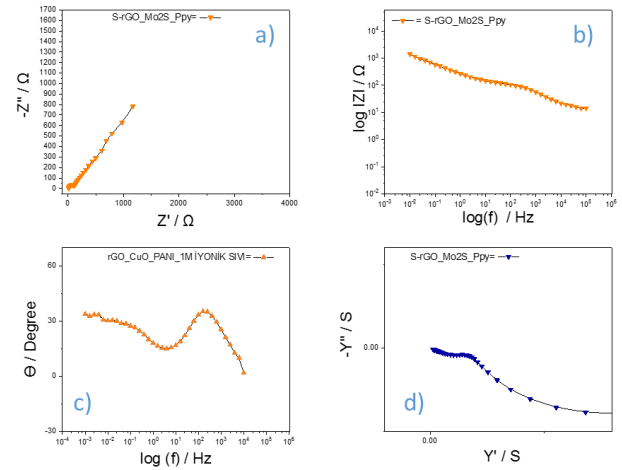


Fig. 6 EIS plots of S-rGO/MoS₂/PPy nanocomposite a) Nyquist plot, b) Bode-magnitude plot, c) Bode-phase plot, d) Admittance plot.

EIS plots of S-rGO/MoS₂/PPy nanocomposites were given in Figure 6. Specific capacitance was obtained as $C_{sp} = 0.276 \text{ F} \times \text{g}^{-1}$ from Nyquist plot. Double layer capacitance and phase angle were obtained as $C_{dl} = 0.187 \text{ F} \times \text{g}^{-1}$ and $\theta = 37.57^\circ$ at 201.86 Hz from Bode-magnitude and Bode-phase plots, respectively. Admittance plots defined conductivity of nanocomposite material ($Y' = 0.0084 \text{ S}$, $Y'' = 0.00168 \text{ S}$) (Fig.6).

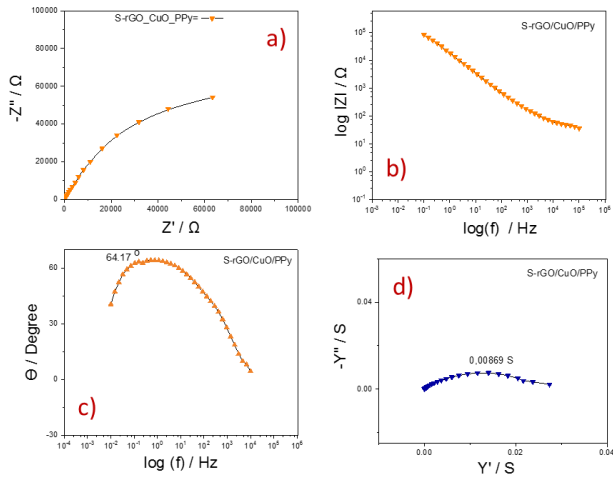


Fig. 7 EIS plots of S-rGO/CuO/PPy nanocomposite a) Nyquist plot, b) Bode-magnitude plot, c) Bode-phase plot, d) Admittance plot.

EIS plots of S-rGO/CuO/PPy nanocomposites were given in Figure 7. Specific capacitance was obtained as $C_{sp} = 5.07 \times 10^{-4} \text{ F} \times \text{g}^{-1}$ from Nyquist plot. Double layer capacitance and phase angle were obtained as $C_{dl} = 0.0081 \text{ F} \times \text{g}^{-1}$ and $\theta = 64.17^\circ$ at 0.717 Hz from Bode-magnitude and Bode-phase plots, respectively. Admittance plots defined conductivity of nanocomposite material ($Y' = 0.0147 \text{ S}$, $Y'' = 0.00869 \text{ S}$) (Fig.7).

I. Stability tests

The stability plots of the S-rGO/MoS₂/PPy and S-rGO/CuO/PPy nanocomposites for 2032 coin cell were given charge/discharge device performances for 1000 cycles (Fig.8). The first capacitance value after 1000 charge/discharge performances were obtained as 98.82% for S-rGO/MoS₂/PPy nanocomposite electrode and 88.97% for S-rGO/CuO/PPy nanocomposite in ionic liquid in 2032 coin cell.

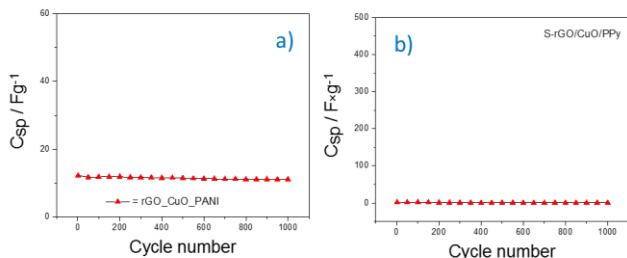


Fig. 8 Stability tests of a) S-rGO/MoS₂/PPy, b) S-rGO/CuO/PPy nanocomposite at a scan rate of $100 \text{ mV} \times \text{s}^{-1}$, 1000 charge-discharge measurements.

IV. RESULTS & DISCUSSION

SupercapBattery device performances were obtained by 2032 coin cell. The highest energy and power densities were obtained for S-rGO/MoS₂/PPy nanocomposite as $E = 2.63 \text{ Wh} \times \text{kg}^{-1}$ at 10 mA and $P = 966.92 \text{ W} \times \text{kg}^{-1}$ at 10 mA. EIS data were also presented as $\theta = 37.57^\circ$ at 201.86 Hz and 98.82% for initial capacitance preservation for 1000 charge-discharge measurements. However, The highest energy and power densities were obtained for S-rGO/CuO/PPy nanocomposite as $E = 1.87 \text{ Wh} \times \text{kg}^{-1}$ at 2 mA and $P = 134.95 \text{ W} \times \text{kg}^{-1}$ at 2 mA. EIS data were also presented as $\theta = 64.17^\circ$ at 0.717 Hz and 88.97% for initial capacitance preservation for 1000 charge-discharge measurements.

V. CONCLUSION

Our results have demonstrated that S-rGO/MoS₂/PPy nanocomposite will be considered as a promising symmetrical electrode materials for the next generation of supercapacitor applications. Our target is to focus on the overall SupercapBattery device performance in energy storage applications in portable and wearable electronic, transport, electrical and hybrid vehicles.

ACKNOWLEDGMENT

Author thank to TUBITAK, Teydeb-1512 project for material and device support. Author also thanks to E. Gul and F. Nacak for their contribution of the laboratory studies.

REFERENCES

- [1] J. Guo, D. Jiang, Y. Zhou, P. Hu, Z. Lin, Y. Liang, "Energy storable VSC-HVDC system based on modular multilevel converter", *International Journal of Electrical Power@ Energy Systems*, vol. 78, pp. 269-276, 2016.
- [2] C. Abbey, G. Joos, "Supercapacitor energy storage for wind energy applications", *IEEE Trans Ind Appl.*, vol. 43, pp. 769-775, 2007.
- [3] L. Maharjan, S. Inoue, H. Akagi, "A transformer less energy storage systems based on a cascade multilevel PWM converter with star configuration", *IEEE Trans Ind Appl.*, vol. 44, pp.1621-1629, 2008.
- [4] Y.H. Hwang, S.M. Lee, Y.J. Kim, Y.H. Kahn, K. Lee, "A new approach of structural and chemical modification on graphene electrodes for high-performance supercapacitors", *Carbon*, vol. 100, pp. 7-15, 2016.

- [5] M. Zhou, F. Pu, Z. Wang, S. Guan, "Nitrogen-doped porous carbons through KOH activation with superior performance in supercapacitors", *Carbon*, vol. 68, pp.185-194, 2014.
- [6] S. Dutta, A. Bhaumil, K.C.W. Wu, "Hierarchically porous carbon derived from polymers and biomass: effect of interconnected pores on energy applications", *Energy Environ. Sci.*, vol. 7, pp. 3574-3592, 2014.
- [7] P. Simon, Y. Gogotsi, "Materials for electrochemical capacitors", *Nat. Mater.*, vol. 7, pp. 845-854, 2008.
- [8] I.U. Hassan, H. Salim, G.A. Naikoo, T. Awan, R.A. Dar, F. Arshad, M.A. Tabidi, R. Das, W. Ahmed, A.M. Asiri, A.H. Qurashi, "A review on recent advances in hierarchically porous metal and metal oxide nanostructures as electrode materials for supercapacitors and non-enzymatic glucose sensors", *J. Saudi Chem. Soc.*, vol. 25, Article number: 101228, 2021.
- [9] A. Huang, Y. He, Y. Zhou, Y. Zhou, Y. Yang, J. Zhang, J. Yang, "A review of recent applications of porous metals and metal oxide in energy storage, sensing and catalysts", *J. Mater. Sci.*, vol. 54, pp. 949-973, 2019.
- [10] M. Inagaki, H. Konno, O. Tanaike, "Carbon materials for electrochemical capacitors", *J. Power Sources*, vol. 195, pp. 7880-7903, 2010.
- [11] Y.Z. Liu, Y.F. Li, Y.G. Yang, Y.F. Wen, M.Z. Wang, "A one-pot method for producing ZnO-graphene nanocomposites from graphene oxide for supercapacitors", *Scripta Materilia*, vol. 68, pp. 301-304, 2013.
- [12] J.Y. Wang, Z.Q. Li, G. Fan, H.H. Pan, Z. Chen, D. Zhang, "Reinforcement with graphene nanosheets in aluminum matrix composites", *Scripta Mater.*, vol. 66, pp. 594-597, 2012.
- [13] Y.Z. Liu, Y.F. Li, Y.G. Yang, Y.F. Wen, M.Z. Wang, "Reduction of graphene oxide by Thiourea", *J. Nanosci. Nanotechnol.*, vol. 11, pp. 10082-10086, 2011.
- [14] Y.F. Li, Y.Z. Liu, W.Z. Shen, Y.G. Yang, Y.F. Wen, M.Z. Wang, "Graphene-ZnS quantum dot nanocomposites produced by solvothermal route", *Mater. Lett.*, vol. 65, pp. 2518-2521, 2011.
- [15] X.L. Ma, G.Q. Ning, Y.F. Kan, Y.M. Ma, C.L. Qi, B. Chen, Y.F. Li, X.Y. Lan, J.S. Gao, "Synthesis of S-doped mesoporous carbon fibres with ultra-high S concentration and their application as high performance electrodes in supercapacitors", *Electrochim. Acta*, vol. 150, pp. 108-113, 2014.
- [16] X.T. Sun, W.T. Shi, L. Xiang, W.C. Zhu, "Controllable synthesis of magnesium oxysulfate, Nanowires with different morphologies", *Nanoscale Res. Lett.*, vol. 3, pp. 386-389, 2008.
- [17] W.J. Si, J. Zhou, S.M. Zhang, S.J. Li, W. Xing, S.P. Zhua, "Tunable N-doped or dual N, S-doped activated hydrothermal carbons derived from human hair and glucose for supercapacitor applications", *Electrochim. Acta*, vol. 107, pp. 397-405, 2013.
- [18] N.H.A. Rosli, K.S. Lau, T. Winie, S.X. Chin, C.H. Chia, "Synergistic effect of sulfur-doped reduced graphene oxide created via microwave-assisted synthesis for supercapacitor applications", *Diamond & Related Materials*, vol. 120, Article number: 108696, 2021.
- [19] M. Vinita, G. Velraj, "Synthesis and characteristic studies on pure and nano silver oxide-doped polypyrrole for supercapacitor application", *J. Mater. Sci: Mater. Electron.*, 33, 6627-6635, 2022.
- [20] Q. Wang, Y. Zhang, J. Xiao, H. Jiang, T. Hu, C. Meng, "Copper oxide / Coprous oxide / hierarchical porous biomass-derived carbon hybrid composites for high-performance supercapacitor electrode", *J. Alloys Comps.*, vol. 782, pp. 1103-1113, 2019.
- [21] D. Majumdar, S. Ghosh, "Recent advancements of copper oxide based nanomaterials for supercapacitor applications", *J. Energy Storage*, vol. 34, Article number: 101995, 2021.
- [22] T.K.S. Wong, S. Zhuk, S. Masudy-Parah, G.K. Dalapati, "Current status and future prospects of copper oxide heterojunction solar cells", *Materials*, vol. 9, Article number:271, 2016.
- [23] R. Tamita, Z. Pu, M.A.T. Kamegawa, S. Higashimoto, "Photochemical properties of copper oxide (CuO) influenced by work functions of conductive electrodes", *Res. Chem. Intermed.*, vol. 45, 5947-5958, 2019.
- [24] T. Pandiyarajan, R. Udayabhaskar, S. Vignesh, R. Arthur, J. Karhikeyan, B. Karhikeyan, "Synthesis and concentration dependent antibacterial activities of CuO nanoflakes", *Mater. Sci. Eng. C.*, vol. C33, pp. 2020-2024, 2013.
- [25] D.Q. Chu, B.G. Mao, L.M. Wang, "Micro-emulsion-based synthesis of hierarchical 3D flower like CuO nanostructures", *Mater. Lett.*, vol. 105, pp. 151-154, 2013.
- [26] K. Mageshwari, R. Sathyamoorthy, "Flower-shaped CuO nanostructures: synthesis, characterization and antimicrobial activity", *J. Mater. Sci. Technol.*, vol. 29, pp. 909-914, 2013.
- [27] M. Vinita, G. Velraj, "Synthesis and characteristic studies on pure and nano silver oxide-doped polypyrrole for supercapacitor application", *J. Mater. Sci: Mater. Electron.*, vol. 33, pp. 6627-6635, 2022.